MCT1-mediated transport of a toxic molecule is an effective strategy for targeting glycolytic tumors

Kivanc Birsoy,[1,2] Tim Wang,[1,2,3] Richard Possemato,[1,2] Omer H. Yilmaz,[1,2] Catherine E. Koch,[1,2] Walter W. Chen,[1,2] Amanda W. Hutchins,[1,2] Yetis Gultekin,[1,2] Tim R. Peterson,[1,2] Jan E. Carette,[1,6] Thijn R. Brummelkamp,[1,7] Clary B. Clish,[3] and David M. Sabatini[1,2,3,4,5]

[1]Whitehead Institute for Biomedical Research, Nine Cambridge Center, Cambridge, MA 02142, USA.

[2]Department of Biology, Massachusetts Institute of Technology (MIT), Cambridge, MA 02139, USA.

[3]Broad Institute, Seven Cambridge Center, Cambridge, MA 02142, USA.

[4]David H. Koch Institute for Integrative Cancer Research at MIT, 77 Massachusetts Avenue, Cambridge, MA 02139, USA.

[5]Howard Hughes Medical Institute, MIT, Cambridge, MA 02139, USA.

[6]Current address: Department of Microbiology and Immunology, Stanford University School of Medicine, Stanford, CA 94305, USA.

[7]Current address: Department of Biochemistry, Netherlands Cancer Institute, Plesmanlaan 121 1066 CX, Amsterdam, The Netherlands.

To whom correspondence should be addressed. Email: sabatini@wi.mit.edu

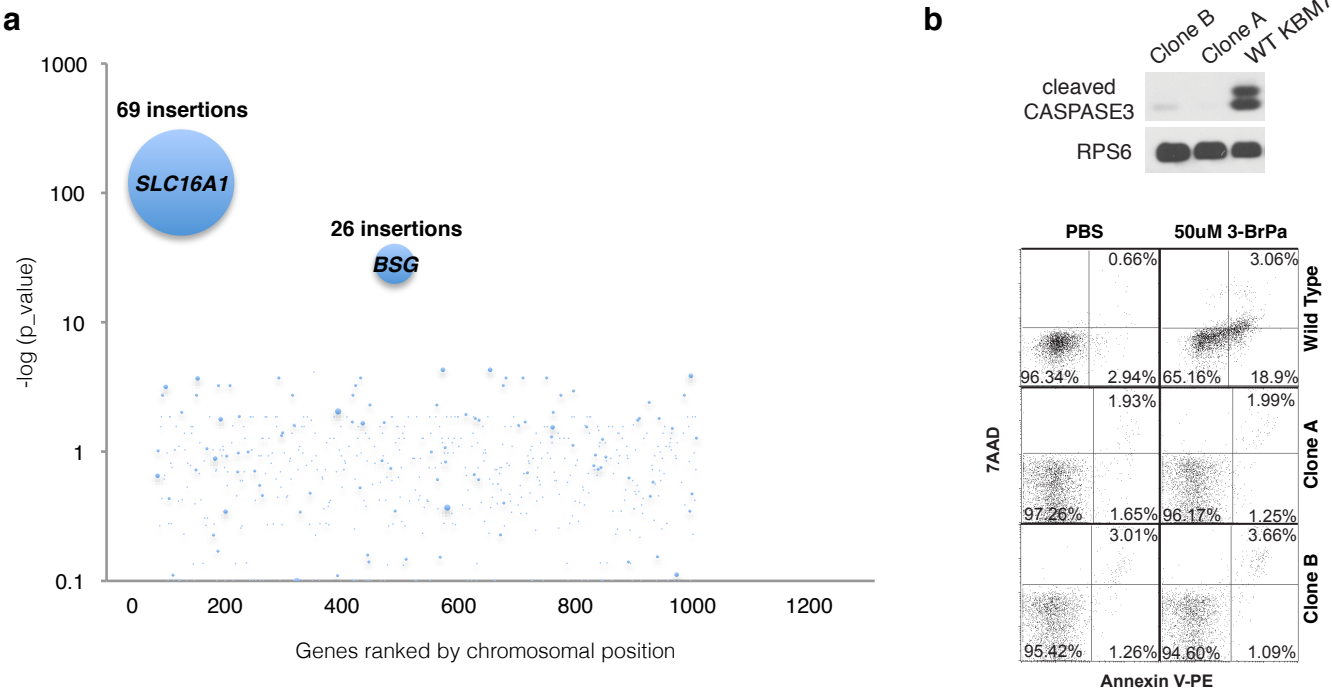

Supplementary Figure 1 - Loss of *SLC16A1* and *BSG* prevents 3-BrPA induced cell death.

a. *SLC16A1* and *BSG* genes contain the highest degree of insertional enrichment in 3-BrPA selected cells compared to the unselected control cells (p=4.7E-121 and p=5E-29, respectively). Y axis represents the inverse logarithm of p values, calculated by Fisher Exact Test. The X-axis represents the insertion sites ordered by their genomic position. The diameter of the bubbles denotes the number of insertions for each gene.
b. Wild type and MCT1 null KBM7 cells were treated for 3 hours with 3-BrPA (50uM) and FACS analysis have been performed using 7AAD and Annexin V staining.

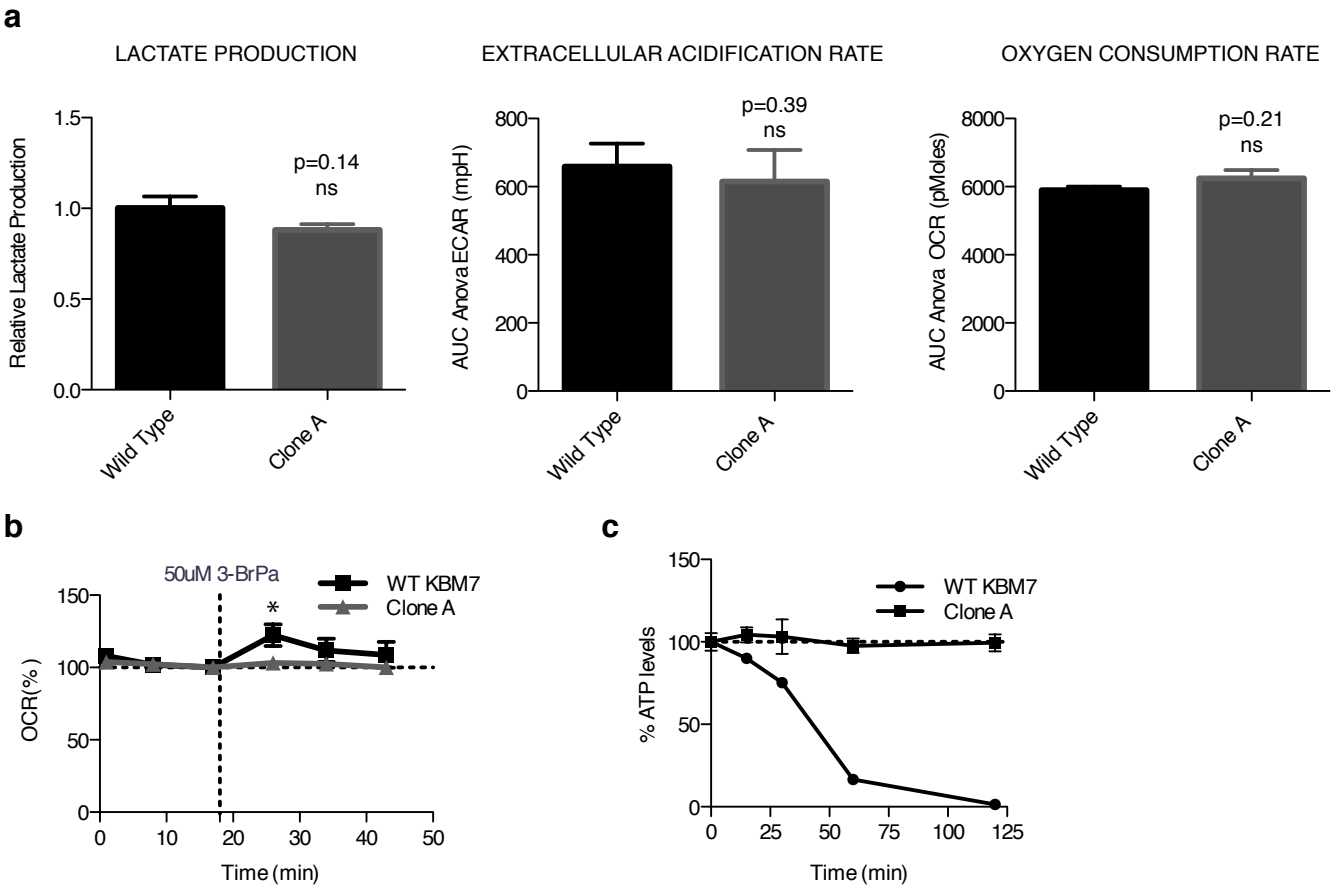

Supplementary Figure 2 - Metabolic characterization of Wild Type and MCT1 null KBM7 cells

a. Lactate production of wild type and MCT1 null KBM7 cells were measured using a colorimetric assay and normalized by cell number. ECAR and OCR reading were measured using Seahorse Extracellular Flux Analyzer. AUC (area under curve) converts OCR rate data to accumulation of total oxygen consumed upon three separate readings.
b. Extracellular Flux Analysis of wild type and MCT1 null KBM7 cells upon 3-BrPA (50 uM) addition. Changes in OCR, a proxy for oxygen consumption, were monitored upon the addition of 50 uM 3-BrPA. Results are displayed as a percentage of the OCR reading immediately before 3-BrPA addition. Error bars are SEM.
c. Relative cellular ATP levels during a time course following 3-BrPA treatment. 50uM 3-BrPA was added onto wild type and MCT1 null KBM7 cells. Relative ATP levels were measured using a luciferase based assay for 2 hours. Error bars are SEM.

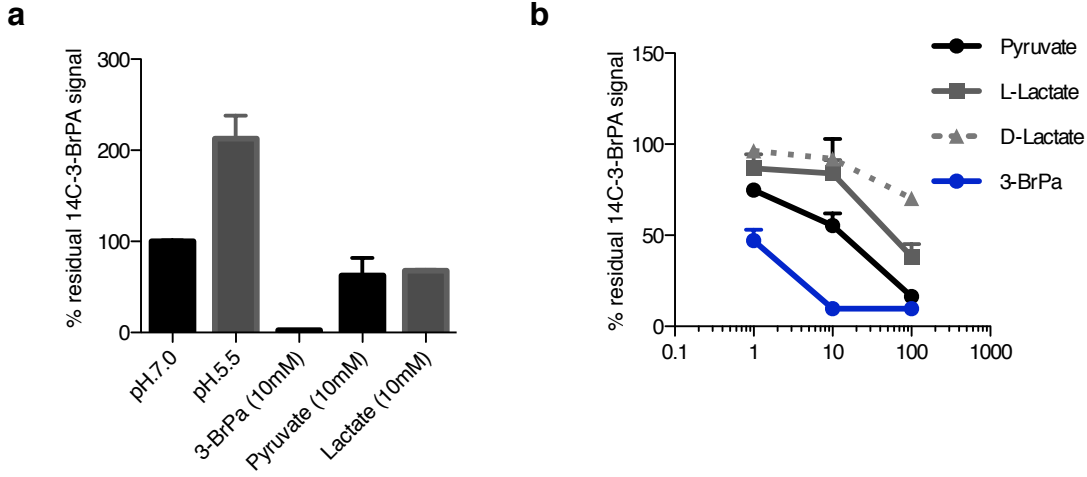

Supplementary Figure 3 - Pyruvate and Lactate can compete with 3-BrPA uptake in KBM7 cells.

a. pH dependence of MCT1 mediated 3-BrPA transport. Wild Type KBM7 cells were incubated with 100 uM of radiactively labeled 3-BrPA for 20 minutes in HBSS in presence of indicated pH conditions and various monocarboxylates (n=3).

b. Dose dependent inhibition of labeled 3-BrPA transport by D-Lactate, L-Lactate and Pyruvate. Wild Type KBM7 cells were incubated with 100 uM radiactively labeled 3-BrPA for 20 minutes in presence of different concentrations of indicated monocarboxylates.

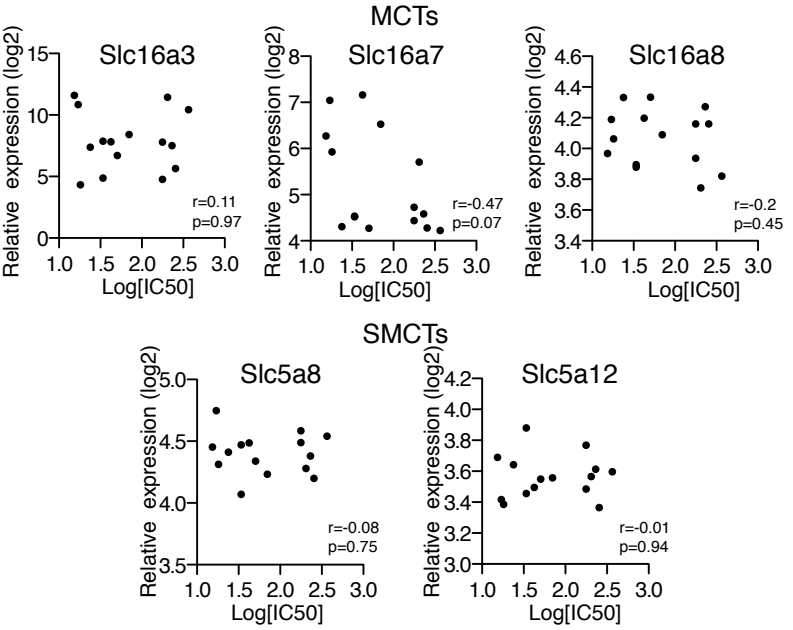

Supplementary Figure 4 - Correlation of other MCT transporter expression levels with 3-BrPA sensitivity

The concentration of 3-BrPA at which 50% cell growth inhibition occurred after 3 days of administration (IC50) was determined for a panel of cancer cell lines. These values were correlated with transcriptome-wide mRNA expression data from the Cancer Cell Line Encyclopedia (CCLE) and the resulting Pearson correlation coefficients were plotted. Relative expression levels for known lactate transporters (MCTs and SMCTs) were correlated with the corresponding IC50 values for 3-BrPA of each cell line.

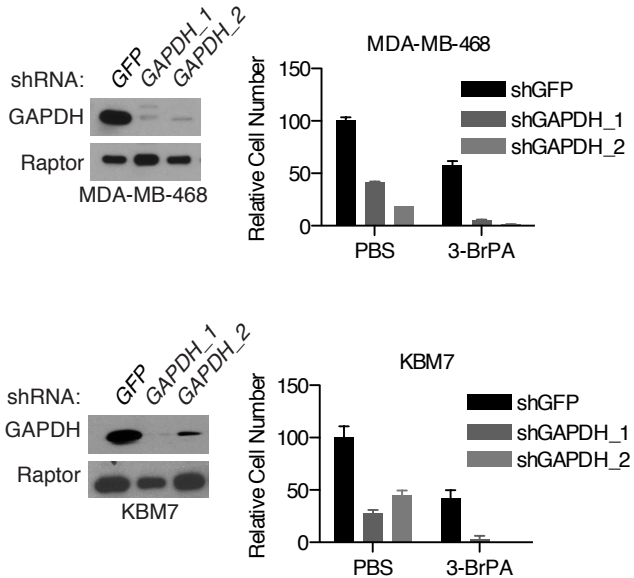

Supplementary Figure 5 - Effect of GAPDH silencing on 3-BrPA sensitivity

Silencing GAPDH expression in cancer cell lines using RNAi causes a decrease in cell proliferation. Cells were infected with corresponding shRNAs and grown in RPMI media in presence and absence of 3-BrPA. 50uM and 10uM 3-BrPA were used for MDA-MB-468 and KBM7, respectively. Note the synergistic effect of GAPDH inhibition and 3-BrPA treatment on cell number.

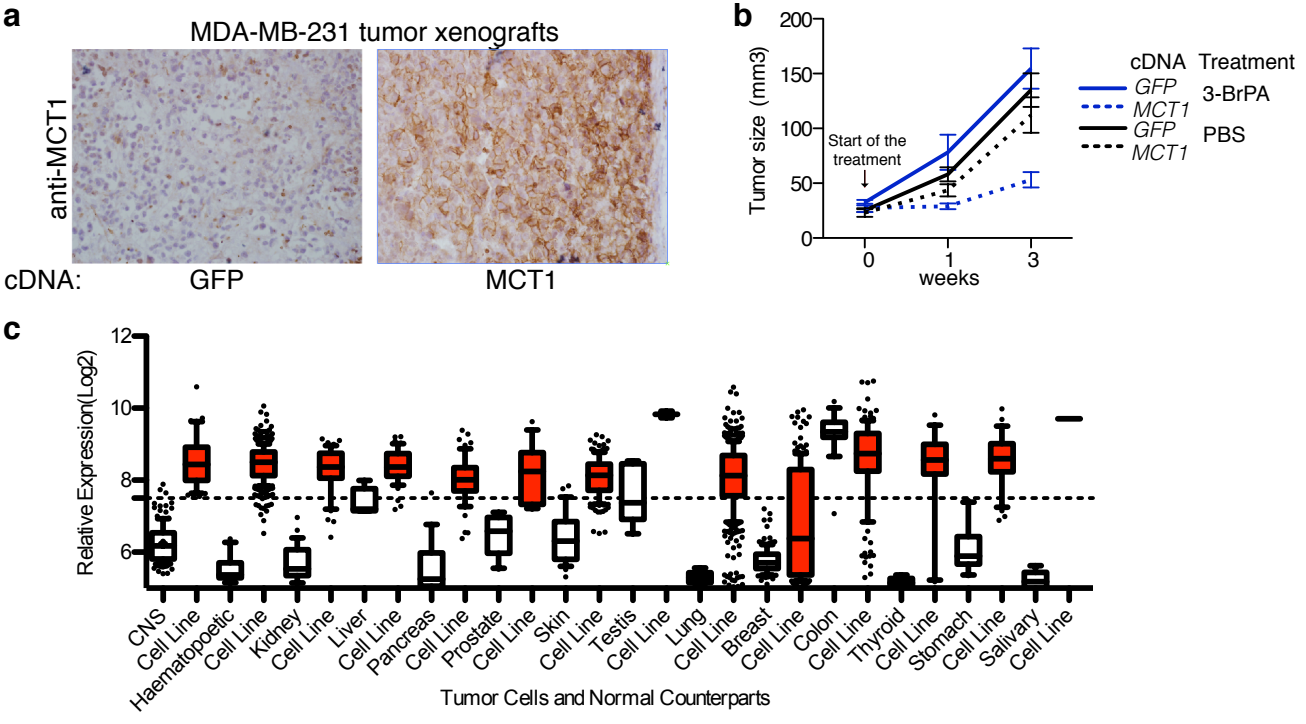

d

Low OCR/ECAR		High OCR/ECAR	
TIMP2	PIM1	FN3KRP	CATSPERB
C12orf75	ORAI2	HS6ST3	ALDH3B2
CLIP4	TNFAIP3	PPP2R2C	KIAA1324
RNF145	SCHIP1	ST6GALNAC2	GPR81
UBE2E3	TBC1D1	TMEM141	MUM1L1
BCAP29	PRKD3	SLC25A21	UCK1
TSPAN3	SLC16A1	ZNF350	MYRIP
NAB1	PDLIM1	LOC150622	ANKRD30A
BET1	PDE8A	CRAT	UMODL1
TMEM55A	C20orf30	BRF1	MUCL1
MDFIC	CTSC	GLS2	WDR85
KLHL5	ROCK2	CNTNAP2	RAB3D
GSTP1	SGCB	ZNF485	PATZ1
LTBP4	IFNAR2	NRK	ZNF480
C6orf145	ANXA11	CLCA2	ZMYND19
CLN5	MTMR2	AR	ZNF90
PGM1	MFGE8	BDH1	RET
PRKAA1	CDK6	RNF208	LOC643072
IFT57	TYW3	LOC254559	AKT1
BRI3	LDHB	CEBPA	ALDH4A1

Supplementary Figure 6 - MCT1 expression in cancers

a. IHC staining of MDA-MB-231 tumors expressing GFP and MCT1 cDNAs using an anti-MCT1 antibody.
b. Time course weight measurements of tumors formed by MDA-MB-231 cells expressing the MCT1 or GFP cDNA during 3 weeks of treatment with vehicle or 3-BrPA (8 mg/kg). Error bars are ± SD (n = 5).
c. Relative expression of MCT1 in cancer cell lines and their normal tissue of origins. Data was collected from CCLE and GEO browser and quantile normalized.
d. Top 40 genes correlating with low (glycolytic) and high (OXPHOS) OCR/ECAR values.

Supplementary Table 1 - Primer Sequences

Cloning vector	Forward Primer	Reverse Primer
pMXs-IRES-blasticidin	AGGGATCCATGCCACCAGCAGTTGGAGG	AGGCGGCCGCTCAGACTGGACTTTCCTCCTCCTTG
PLJM1-puro	ATTGAATTCTATGCCACCAGCAGTTGGAGG	ATTAATTCGTTCGAATCAGACTGGACTTTCCTCCTCCTTG